New Electrical System for Water Desalination Plant: Design and Modeling of a Linear Permanent Magnet Generator for Tidal Energy Conversion

El Manaa Barhoumi *, **‡, Youcef Berrouche*

* Department of Electrical Engineering, College of Engineering, Majmaah University, 11952, Saudi Arabia

** Université de Tunis El Manar, Ecole Nationale d'Ingénieurs de Tunis, Laboratoire Analyse, Conception et Commande des Systèmes (LR11ES20)

(e.barhoumi@mu.edu.sa, y.berrouche@mu.edu.sa)

‡ Corresponding Author; El Manaa Barhoumi, Department of Electrical Engineering, College of Engineering, Majmaah University, 11952, Saudi Arabia, Tel: +966 53 492 9856,

e.barhoumi@mu.edu.sa

Received: 16.04.2017 Accepted:14.05.2017

Abstract- This article presents the design and the modelling of a new linear generator to convert the tidal energy to electrical energy. This machine will be used in a renewable energy power station. The power station using tide energy will produce electrical energy for the supply of equipment used in water desalination plant in Saudi Arabia. Moreover, the tidal energy can produce more electrical energy than the photovoltaic and the wind power. A new electrical machines and power converters should be designed to convert wave energy to electrical power. In this paper, sizing and simulations of a new linear generator are carried out using Finite Element Method. The simulation of linear generators with power converters shows the efficiency of the proposed system for tidal energy conversion.

Keywords Tidal Energy, Electromagnetic analysis, Linear Generator, Power converter

1. Introduction

The world faces many problems related to the needs of water. Many countries developed and installed water desalination plants [1]. These plants produce pure water from the sea water. Hence, they participated considerably to solve the water problems in these countries [2]. The electrical energy required to run the different equipment in the desalination power plant is generally produced by conventional power plants of electrical energy; thermal and nuclear power stations. In the last decade, the photovoltaic and the wind power energy are more used to produce electrical power around the world. In Saudi Arabia, the water desalination plant in Al Khafji city requires more than 6 GWh of electrical energy. Photovoltaic systems are installed to produce approximately the half of required power [3]. The sustainable energy outlook for Saudi Arabia by 2050 shows a concentration on photovoltaic and wind power energy as main sources of renewable energy. However, the tide energy in Saudi Arabia can produce more electrical energy than both wind power and photovoltaic [4], [5]. Usually the desalination techniques are typically very energy intensive. The references show that energy consumption can account for up to 70 percent of the desalination station cost [1], [6]-[8]. Indeed, the global production of fresh water around the word uses approximately 72.2 terawatt-hours of electricity per year [14]. Identify novel ways to reduce the cost of electricity consumption for water desalination is the goal of this challenge. This task can be achieved either through novel technology advances, process improvements, or both. Many electromechanical systems to produce electrical energy from tide energy are studied and proposed in references [9]-[11]. These systems can be classified in two types. The first one is based on the utilization of classical rotary machine [12]-[14]. However, the second type uses new linear machines designed especially for this type of application [15]-[17]. The objective of this paper is to propose and study a new linear machine characterized by its simplicity of construction. This machine is different to conventional machines. Double stator is used to increase the maximum power produced. Indeed, tubular structures of linear generators were studied. In this paper, the generator has a plane structure. This makes the construction of the machine easy.

This paper is organized as follow. The water desalination plant is presented in section 2. Section 3 concerns the design and the analysis of the efficiency of the new linear generator. Discussion of the reliability of the project is given in

section4. Conclusions and perspectives are summarized in section 5.

2. The Water Desalination Plant

The proposed study focuses on Al Khafji desalination plant. This plant was builted in Al Khafji City located to the north-eastern part of the Kingdom of Saudi Arabia near the State of Kuwait border. The desalination plant will be able to supply 60,000m³ of desalinated seawater per a day to the city of Al Khafji in north-eastern Saudi Arabia [3]. According to research published on energy required for water desalination plant, 100 MWh are required to produce 10 km3 of fresh water. Then, the water desalination plant at Al Khafji requires approximately 6 GWh to produce 60 km3 of water. The water desalination plant will provides a regular supply of water to the region throughout the year. The system employs the new Solar Saline Water Reverse Osmosis (Solar SWRO) desalination method using ultra-filtration (UF) for the pre-treatment process. The using of tidal energy for water desalination plant allows reducing the costs of requested electrical energy for the supply of equipment.

3. Design of the New Linear Generator

3.1. Description of the linear generator

In the last decade many renewable energy power systems were proposed. In some projects, tidal energy is used alone. Usually, hybrid systems based on tidal, photovoltaic and wind power are used. Fig. 1 shows a small renewable energy hybrid system using tidal energy in addition to photovoltaic and wind power. To increase the efficiency of such systems, efficient linear generator should be designed to produce the maximum of electrical energy from tidal energy. The aim of this section is to present the design of a new linear generator working by tide energy. This linear generator can be installed to produce electrical energy alone or in hybrid renewable energy system.

Fig.1. Small Renewable Energy Hybrid System 500 W

Figure 2 shows a 3D view of the proposed linear generator. For the linear generator in this study, the mover part is formed by only permanent magnets (NdFe35) that will be integrated with a lightweight non-ferromagnetic material such as aluminum. In this configuration, no overlap exists between two adjacent permanent magnets. The magnetic separation between each two adjacent permanent magnet is equal to the tooth width. These permanent magnets are placed in way to make the best circulation of the magnetic flux in the magnetic circuit of the stator. In this machine, the stator is formed by two parts where each one is composed by a three phases. For the core material, the steel 1010 with a nonlinear BH curve is used.

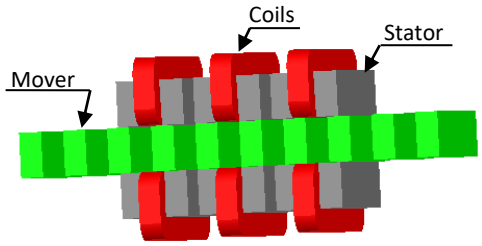

Fig. 2. 3D View of the linear double stator generator

The mover of the linear generator is able to make a displacement in the two directions. Indeed, tidal energy should be exploited completely. This allows the production of electrical energy during the two directions of movement. Hence, to ensure the reversibility and the regularity of operation of the linear generator, 2 conditions must be satisfied. The use of equal tooth widths on the mover and on the stator is indispensable. On the other hand, the slot width must be equal to the tooth width. Hence, for the proposed actuator, the tooth and slot widths are given by:

$$T_w = S_w = 50\,mm \tag{1}$$

The non-ferromagnetic separation between each two adjacent phases is equal to the third of mechanical displacement period. The mechanical period is equal to the distance token by the mover to move between two successive unaligned or aligned positions. The tooth pitch is calculated using the following expression:

$$\lambda = 2T_w = 100\,mm \tag{2}$$

The air gap should be selected so as to guarantee a maximum induced voltage and taking into account the mechanical construction difficulties. The slot depth is selected so as to place the stator windings. The geometrical dimensions of the actuator are given in Fig. 3, which provides a view of an elementary portion of the linear generator. The mechanical and electrical parameters of the actuator obtained after the analytical design combined with the finite element method are summarized in Table 1.

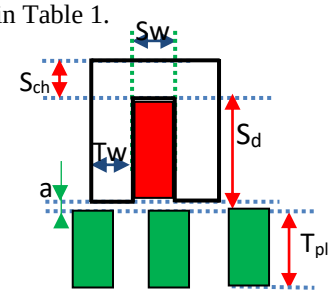

Fig.3. Geometrical dimensions of the linear generator

Table 1. Main parameters of the linear generator

Quantity	Symbol	Values
Tooth width	Tw	50 mm
Air gap width	e	1 mm
Slot depth	Sd	100 mm
Translator thickness	Tt	300 mm
Translator pole length	Tpl	100 mm
Maximum electrical Current	I	24 A
Turns per phase	N	695

3.2. Finite Elements Analysis

The Finite Element Method (FEM) is usually used when precise design and simulations of electrical devices are required. Indeed, the FEM allows determining precisely the different output variables such as the magnetic flux, the magnetic inductance [18], [19]. Hence, the evaluation of the linear generator electromagnetic characteristics will be carried out with a numerical field analysis using the FEM software Maxwell-2D. The proposed generator's geometrical structure is simple and not complicated. For this reason, a 2D FEM analysis is considered sufficient. The computational domain introduced in the software is represented by a cross section of the linear generator and the regions are meshed, as shown in Fig.4. To obtain precise FEM results, the density of the mesh elements must be sufficient. On the other hand, increasing the number of elements increases the computation time [20]. Consequently, the mesh is a choice, taking into account the necessity of the accurate results and an acceptable computation time.

To calculate the magnetic flux and others electromagnetic characteristic of the linear machine, magneto static type of problem is fixed. To solve the problem, the magneto static field will be calculated at each iteration. The governing differential equation to be solved in the 2D FEM is [10]:

$$\frac{\partial}{\partial x}\left(\frac{1}{\mu}\frac{\partial A_z}{\partial x}\right)+\frac{\partial}{\partial y}\left(\frac{1}{\mu}\frac{\partial A_z}{\partial y}\right)=-J_z \qquad (3)$$

To find the magnetic flux and inductance, the Finite Element Method software computes the magnetic potential field A. To verify certain previously requirements such as the distribution of the magnetic field on the generator structure, the magnetic field distribution is plotted to analyze the saturation of the actuator. The flux lines produced in the mover part by the permanent magnet are canalized into the magnetic circuit of the stator as shown in Fig.5, 6 and 7. Due to the movement of the mover, an induced voltage will be produced according to Lenz low. Fig.5. shows the distribution of the magnetic flux produced by the permanent magnets placed on the mover. For each phase, the flux is maximum at the aligned position. Indeed, at the aligned position, all the flux produced by the permanent magnet aligned with the stator poles is conducted by the magnetic circuit of the stator. At the unaligned position, the flux takes its minimum values as shown in Fig.7. The most quantity of the generated flux is canalized through the slots of the stator. Fig.8. shows the approximation of the variation of the magnetic flux in one phase of the stator. The assumption supposes a linear variation of the flux between the aligned and the unaligned position.

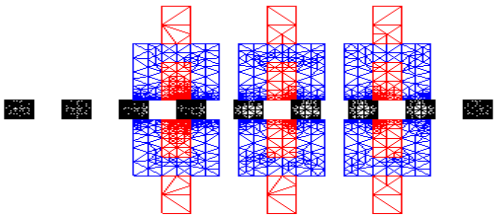

Fig. 4. Meshing of the double stator linear generator

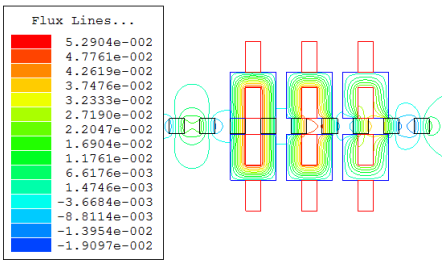

Fig. 5. Poles of phase A aligned with the mover poles

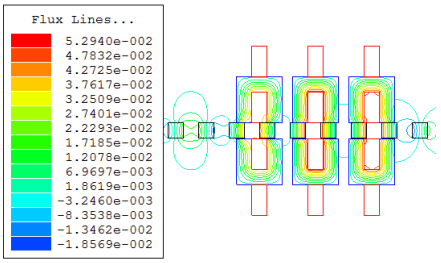

Fig.6. Poles of phase A in intermediate position with the mover poles

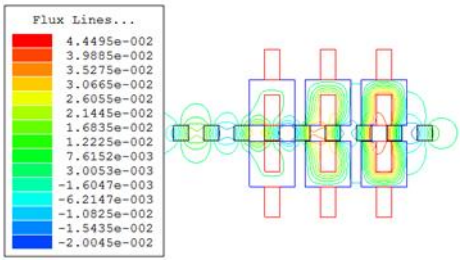

Fig.7. Poles of phase A unaligned with the mover poles

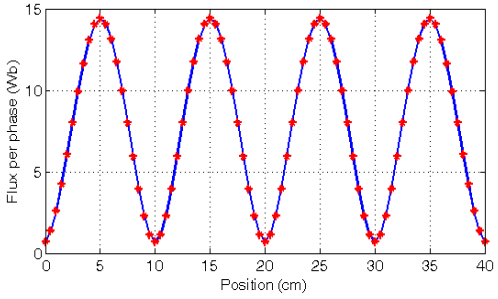

Fig.8. Variation of magnetic flux of phase A

The induced voltage produced due to the movement of the mover is proportional to the number of turns per coil and the variation of the flux over the time. Hence, the induced voltage depends on the speed of the mover. The induced voltage variation versus the time for different mover speed is shown in Fig.9. Increasing the speed conducts to increasing the induced voltage. Fig.9. shows a maximum induced voltage equal to 155.5V obtained for a speed equal to 0.33m/s. This induced voltage decreases to 40V for a mover speed equal to 0.01m/s. For a mover speed constant and equal to 0.2m/s, the induced voltages are shown in Fig.10.

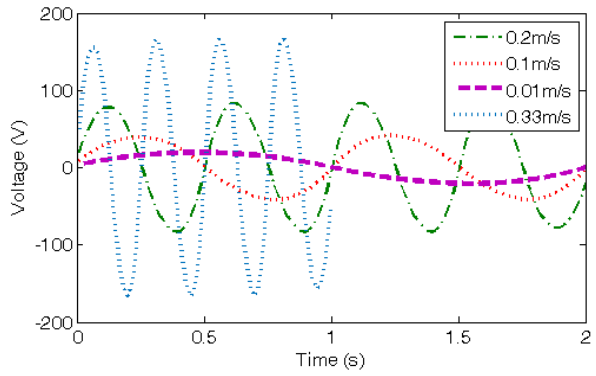

Fig.9. Voltage versus speed of the proposed linear generator

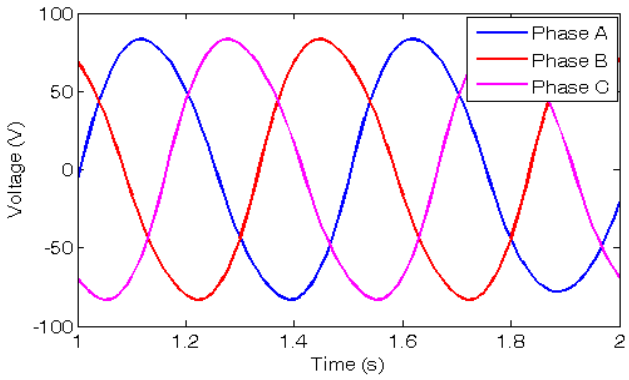

Fig.10. Three phase EMF variation at mover speed of 0.2m/sec

4. Performances Analysis of the Generator

The induced voltage depends to the variation of the flux versus time as it is given:

$$e = -N\frac{d\varphi}{dt} \tag{4}$$

Where N is the number of turns per phase. φ is the partial flux by turn.

The induced voltage is proportional directly to the number of turns per phase. Hence, increasing the number of turns per coil allows increasing the induced voltage. However, this way allows increasing considerably the core losses in the stator by increasing the electrical resistance of each phase. The copper losses are given by:

$$P_C = RI^2 = \rho\frac{l}{A}I^2 \tag{5}$$

Where ρ the copper resistivity, l and A are respectively the length and the section area of the coil wire. The winding current density is defined as:

$$J = \frac{I}{A} \tag{6}$$

Consequently, the copper losses are:

$$P_C = \rho l A J^2 \tag{7}$$

To study the effect of the section of conductor variation on the output power and the copper losses, a simulation were carried out. The results are shown in Fig.11 and Fig.12. Fig.11 shows the variation of the output power versus the conductor's section. When the section increases, the admissible electric current increases. Consequently the produced power increases. However, increasing the electrical current conducts to important copper losses.

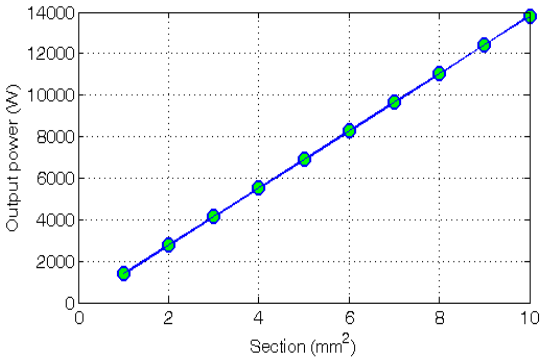

Fig.11. Output Power versus the wire section

The variation of the copper losses versus the electric resistance and the electrical current, presented in Fig.12, shows a big copper losses when the current and the resistance are more than 40 A and 20 Ω respectively. Hence, the section of the conductors should be carefully determined.

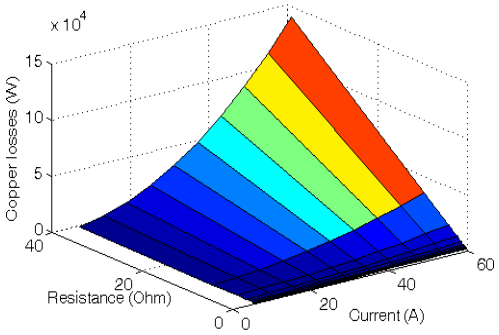

Fig.12. Copper losses versus current and resistance

For a current equal to 24 A and conductor section of 4 mm^2, the resistance is 2.44 Ω and the copper losses are:

$$P_C = 2.4486 \times 24^2 = 1.41kW \quad (8)$$

For the same conductor's section, the output power is about 6 kW as shown in Fig.11. Hence, 4 mm^2 as a conductor's section seems a good choice for the linear generator. Then, the number of turns per coil is 695 turns. The electrical output parameters of the linear generator are given in table.2.

Table.2. Main parameters of the linear generator

Quantity	Symbol	Values
Frequency,	f	60 Hz
Voltage	V	250 V
Electrical Current	I	24 A
Turns per phase	N	695
power	P	6000 W

5. Linear Generator and Power Converter Modeling

5.1. Dynamic model of the linear generator

The voltage in each phase of the linear generator depends to the induced voltage and the current absorbed by the load. Hence, the voltage is given by:

$$u = e - Ri - L\frac{di}{dt} \quad (9)$$

R and L are respectively resistance and inductance per phase. The induced voltage is function of the speed of the mover. Hence the equation (9) will be:

$$u = f(v) \times v - Ri - L\frac{di}{dt} \quad (10)$$

The relation of the induced voltage with the mover speed is modeled by a nonlinear function presented in Fig.11 and Fig.12. Indeed, both the frequency and the maximum voltage vary with the mover speed.

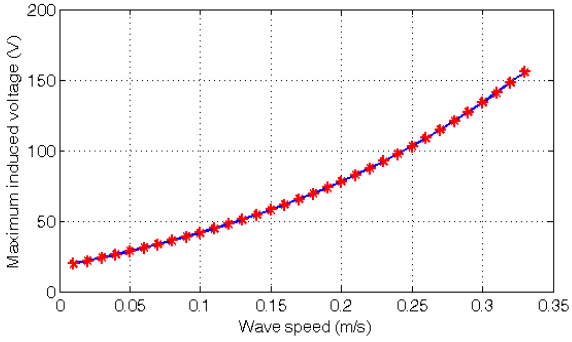

Fig.13. Maximum induced voltage versus mover speed

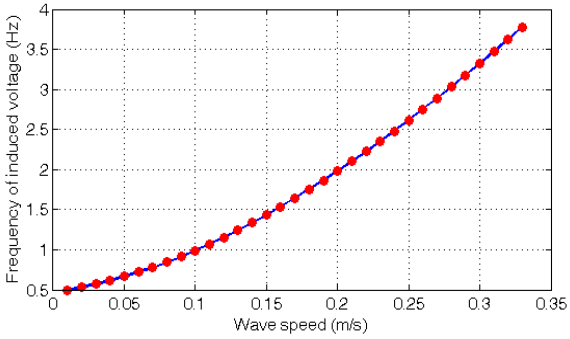

Fig.14. Frequency of induced voltage versus mover speed

According to equations (9) and (10), the model given in Fig.15. is developed and implemented in Matlab- Simulink. The advantage of this dynamic model is to calculate the voltage of the linear generator based to the mover speed and the current absorbed by the load. The variations of both frequency and maximum voltage of the induced voltage are modeled by a look up tables as shown in fig.15.

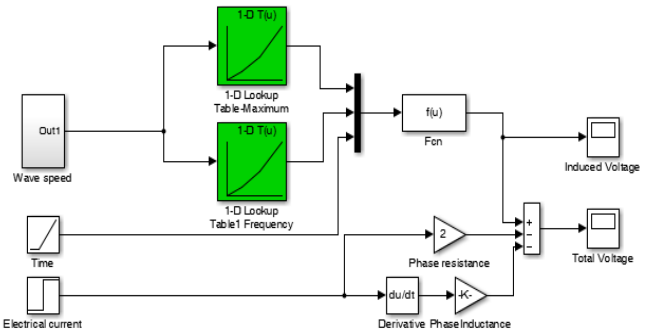

Fig.15. Single phase Simulink model of the linear generator

5.2. Modeling of the power converter

The power converter connected to the linear generator is composed by a rectifier and a Pulse Width Modulation (PWM) inverter. The rectifier is used to convert the variable alternative voltage to direct current voltage. However, the PWM inverter should convert the DC variable voltage to constant AC voltage. For modeling the rectifier, the diodes are assumed ideal and the conduction will be maintained continuous. In this case the model of the converter is realized simply by a functional approach based on commutations functions where the diodes are opened and closed.
The output voltage of the rectifier is given by:

$$v_0 = F_1.v_i - F_2.v_i \quad (11)$$

Where F_1 and F_2 are a commutation functions given respectively by equations (13) and (14):

$$F_1 = \begin{cases} 1 \ if \ v_i \geq 0 \\ 0 \ if \ v_i \ \square \ 0 \end{cases} \quad (12)$$

$$F_2 = \begin{cases} 0 \ if \ v_i \geq 0 \\ 1 \ if \ v_i \ \square \ 0 \end{cases} \quad (13)$$

The model of the rectifier implemented on Matlab-Simulink is shown in Fig. 16.

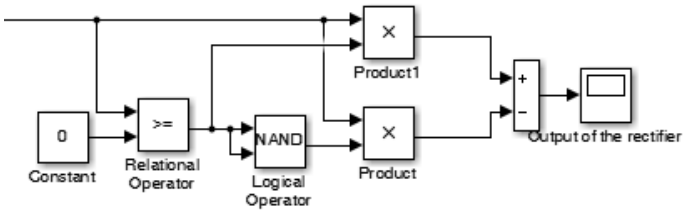

Fig.16. Simulink Model of a single phase uncontrolled rectifier

The simulation of the output voltage of the rectifier for different mover speeds is shown in Fig. 17. The voltage depends directly to the mover speed. It increases when the mover speed increases. Indeed, for three levels of mover speed, 0.2 m/s, 0.3 m/s and 0.4 m/s, the rectifier output voltage varies between 134 V, 238 V and 340 V.

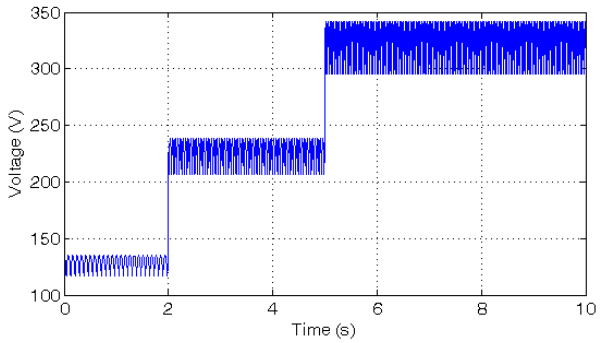

Fig.17. Output voltage of the three phase rectifier for three different mover speeds

For both cases connecting the linear generator to the grid or connecting it the three phases AC loads, the DC output voltage of the rectifier will be converted to AC voltage using three phase inverter.

The line to neutral output voltage of the three phase inverter is given by the following equation:

$$V_{AC} = \frac{V_{DC}}{3}\begin{bmatrix} 2 & -1 & -1 \\ -1 & 2 & -1 \\ -1 & -1 & 2 \end{bmatrix}\begin{bmatrix} c1 \\ c2 \\ c3 \end{bmatrix} \quad (14)$$

Where *c1*, *c2* and *c3* are the PWM control signals of the first three switches of the inverter. Developed Simulink model of the three phase inverter is shown in Fig.18. Where C is the PWM control signal, io and ii are respectively the output and the input currents of the inverter.

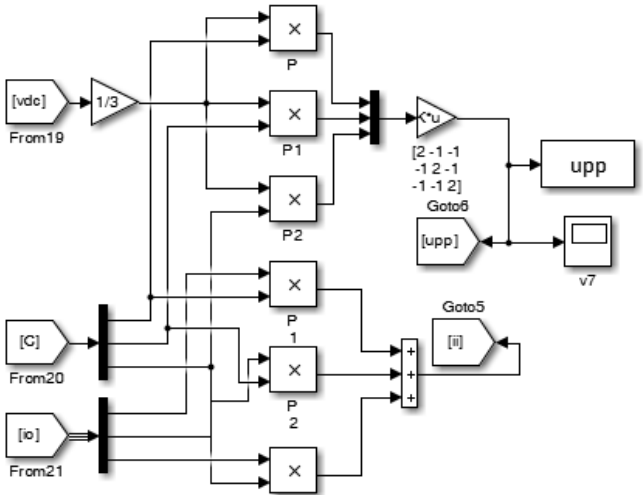

Fig.18. Simulink Model of the three phase inverter

The output voltage of the inverter is shown in Fig.19. The fundamental of the output voltage varies with the input DC voltage according the following expression:

$$U_{Max} = \frac{\sqrt{3}}{2}\frac{V_{m\max}}{V_{t\max}}V_{DC} \quad (15)$$

Where V_{mmax} and V_{tmax} are respectively the amplitudes of the sinusoidal and the triangular voltages of the PWM control signals.

The relation between the amplitude of the sinusoidal voltage and the triangular voltage determines the maximum value of the fundamental line-line voltage of the inverter. However, the frequency is determined by the frequency of the sinusoidal voltage.

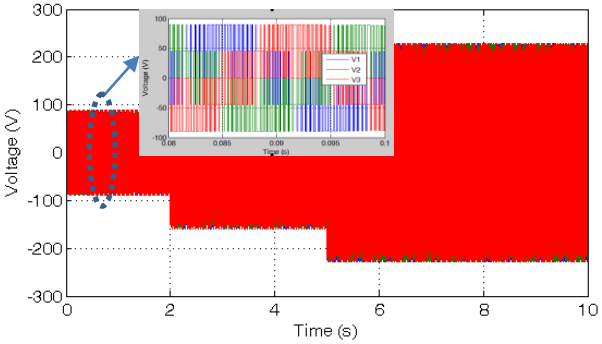

Fig.19. Output voltage of the three phase inverter

6. Discussion of Feasibility and Project efficiency

The electrical energy production depends essentially to the generator mover speed. Indeed, the output voltage of the inverter increases with the speed. The velocity of traveling waves on the ocean is wavelength dependent and for shallow enough depths, the velocity also depends upon the water depth. Wave speed is expressed by the following:

$$v = \sqrt{\frac{g\lambda}{2\pi}\tanh\left(2\pi\frac{d}{\lambda}\right)} \quad (16)$$

Where λ and g are respectively the wavelength and the acceleration gravity. d is the depth of the wave.

The power of the tide depends essentially on the volume of water. The potential energy contained in a volume of water is:

$$E = \frac{1}{2}A\rho g h^2 \quad (17)$$

Where A is the horizontal area of the barrage basin, h is the vertical tidal range, ρ is the density of water, varies between 1021 and 1030 kg per cubic meter, and g is the acceleration due to the Earth's gravity = 9.81m/s^2.

For Al Khafji city located at the north-eastern of Saudi Arabia as shown in Fig. 20, the tidal range of tide is approximately 1.8 m. Considering a surface of the tidal energy amassing plant of 9 km^2, the potential energy is about 146.6 ×10^9 J.

Fig.20. Location of Al Khafji City in Saudi Arabia

According to Fig.21, 2 high tides and 2 low tides appeared daily. At low tide the potential energy is zero. Then, the total energy potential per day is:

$$E_{total} = A\rho g h^2 \quad (18)$$

The mean potential power generation is given by:

$$E_{Average} = \frac{A\rho g h^2}{T} \quad (19)$$

Where T is the time in 1 day. Hence, the mean potential power generation is about 3400 MW

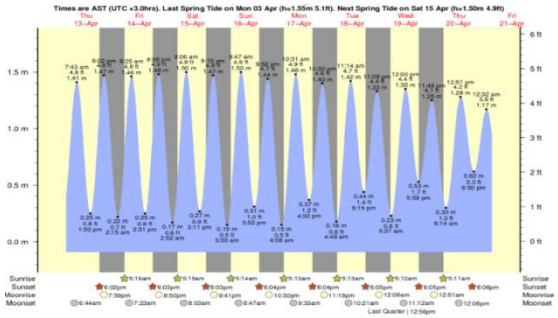

Fig.21. Sea Conditions for Al Khafji-Dammam [21]

7. Conclusion

In this paper, a new linear double stator generator is designed to convert tidal energy to electrical energy. The design was conducted through analytical study coupled with the finite element method. The obtained results of the design show the efficiency of the proposed method of design. The proposed linear generator allows producing about 6kW of electrical energy for 0.2 m/s mover speed.

In the future work, the optimization of the new Linear permanent magnet generator for wave energy conversion will be performed to determine the optimal electrical and geometrical parameters corresponding to the maximum output electrical power. On the other hand, modeling and design of power electronic converters associated with the linear generator will be conducted to control the flow of the electrical energy provided by the new generator.

Acknowledgements

This work is supported by scientific research deanship at Majmaah University, Saudi Arabia under the contract number 37/58.

References

[1] M. B. Baig, A. A. Al Kutbi, Design features of a 20 migd SWRO desalination plant, Al Jubail, Saudi Arabia, Desalination, 118(1) (1998), https://doi.org/10.1016/S0011-9164(98)00068-X

[2] A.G. Maadhah, C.K. Wojcik, Performance study of water desalination methods in Saudi Arabia, Desalination, 39. (1981)

[3] Al Khafji Solar Saline Water Reverse Osmosis (Solar SWRO) Desalination Plant, Saudi Arabia, www.water-technology.net.

[4] F. O. Rourke, F. Boyle, A. Reynolds, Tidal energy update 2009, Applied Energy 87 (2) (2010)

[5] M. E. H. Benbouzid, J. A. Astol, S. Bacha, J. F. Charpentier, M. Machmoum, T. Maitre, D. Roye, Concepts, modeling and control of tidal turbines, Marine Renewable Energy Handbook (2013)

[6] M. Iaissaoui, D. Nehari, D. OUINAS, Analysis of the feasibility of Combined Concentrating Solar Power With Multi Effect Desalination for Algerian Coast, International Journal of Renewable Energy Research-IJRER, Vol 7, No 3 (2017) (article)

[7] Okinda, Victor Omondi, and Nicodemus Abungu Odero. "Modeling, Simulation and Optimal Sizing of a Hybrid Wind, Solar PV Power System in Northern Kenya." International Journal of Renewable Energy Research (IJRER) 6.4 (2016): 1199-1211 (article)

[8] M. Abdollahi, J.I Candela, J. Rocabert; R. S. M Aguilar; J. R. Hermoso, Improving long line stability by integrating renewables using static synchronous generators, IEEE International Conference on Renewable Energy Research and Applications (ICRERA), 2016, Pages: 512 – 517 (Conference Paper)

[9] Y. Cetinceviz, D. Uygun, H. Demirel, Optimal Design and Verification of a PM Synchronous Generator For Wind Turbines, International Journal of Renewable Energy Research-IJRER, Vol 7, No 3 (2017) (article)

[10] T. Honda, K. Kasamura, Y. Nakashima,Y. Nakanishi; H. Higaki, An ideal generation system for streamflow, tidal and ocean currents -Installation of biomimetic sealing system, IEEE International Conference on Renewable Energy Research and Applications (ICRERA), 2015, Pages: 596 – 599 . (Conference Paper)

[11] Y. Nakanishi; Y. Oka; J. Sanderson; T. Honda; K. Kasamura; Y. Nakashima; H. Higaki, Biomimetic sealing system with hydrated materials for ocean current or tidal power generation, IEEE International Conference on Renewable Energy Research and Application (ICRERA), 2014, Pages: 755 – 759 (Conference Paper)

[12] M. Caruso; A. O. Di Tommaso; F. Genduso; R. Miceli; G. Ricco Galluzzo; C. Spataro; F. Viola, Experimental characterization of a wind generator prototype for sustainable small wind farms, IEEE International Conference on Renewable Energy Research and Applications (ICRERA), 2016, Pages: 1202 – 1206. (Conference Paper)

[13] M. Biberoğlu; L. Ovacık, Improving power generation capability of the surface mounted permanent magnet generator using series resonant converter, IEEE International Conference on Renewable Energy Research and Applications (ICRERA), 2016, Pages: 500 – 505 (Conference Paper)

[14] A. Bahaj, L. Myers, Fundamentals applicable to the utilisation of marine current turbines for energy production, Renewable energy 28 (14) (2003)

[15] M. S. Camara, M. B. Camara, B. Dakyo, H. Gualous, Permanent Magnet Synchronous Generator for Offshore Wind Energy System Connected To Grid And Battery-Modeling And Control Strategies, International Journal Of Renewable Energy, 5(2), 2015.

[16] H. Yu, C. Liu, B. Yuan, M. Hu, L. Huang, S. Zhou, A permanent magnet tubular linear generator for wave energy conversion, Journal of Applied Physics 111, (2012).

[17] J. Bard, P. Kracht, Linear Generator Systems for Wave Energy Converters, Fraunhofer IWES, 2013.

[18] E. M. Barhoumi, F. Wurtz, C. Chillet, B. Ben Salah, O. Chadebec, Efficient Reluctance Network Model for Modelling, Design and Optimization of Linear Switched Reluctance Motor, IEEE International Conference COMPUMAG Canada, 2015. (Conference Paper)

[19] E. M. Barhoumi ,F. Wurtz, C. Chillet, B. Ben Salah, and O. Chadebec, Efficient Reluctance Network Formulation for Modeling Design and Optimization of Linear Hybrid Motor, IEEE Trans on Mag, Vol. 52, No. 3, March 2016. (Article)

[20] E. M. Barhoumi, M. Hajji, B. Ben Salah, Design of a double stator linear switched reluctance motor for shunting the railways channels, Turkish Journal of Electrical Engineering & Computer Sciences, Vol. 2 n 22, February 2014. (Article)

[21] Tidal range in Al Khafji [https://www.tide-forecast.com/locations/Dammam/tides/latest]